Int. J. Heat Mass Transfer. Vol. 25, No. 5, pp. 631–641, 1982
Printed in Great Britain

0017–9310/82/050631–11 $03.00/0

FINITE AMPLITUDE CONVECTION IN A POROUS CONTAINER WITH FAULT-LIKE GEOMETRY: EFFECT OF INITIAL AND BOUNDARY CONDITIONS

ROBERT P. LOWELL
School of Geophysical Sciences, Georgia Institute of Technology, Atlanta, GA 30332, U.S.A.
and
HEROEL HERNANDEZ
Chevron Oil Field Research Company, P.O. Box 446, LaHabra, CA 90631, U.S.A.

(*Received* 16 *March* 1981 *and in revised form* 12 *October* 1981)

Abstract—Finite difference techniques have been used to investigate finite amplitude convection in a porous container with fault-like geometry. The principal purpose was to determine the role of wall boundary conditions and the initial perturbation on the subsequent flow pattern. In containers with prescribed wall temperatures, the flow was weakly 3-dim., but with the general appearance of 2-dim. transverse rolls. In containers bounded by impermeable blocks of finite thermal conductivity, a flow pattern similar to that for containers with prescribed wall temperatures tended to be set up; but asymmetric initial perturbations tended to give rise to slowly evolving flows in which asymmetries were still present after 10^4 yr. The results were compared with data from naturally occurring geothermal systems.

NOMENCLATURE

a, thermal diffusivity;
A, $= L_z/L_x$, aspect ratio;
B, $= L_z/L_y$, aspect ratio;
c, specific heat;
g, gravitational acceleration;
K, permeability;
L, dimension of porous zone in direction of subscript;
M, horizontal dimension of impermeable material;
P, pressure;
R, Rayleigh number;
R_c, critical Rayleigh number;
t, time;
T, temperature;
T_0, T_1, temperature at cold and hot boundaries, respectively;
ΔT_0, temperature difference between hot and cold boundaries;
u, v, w, x, y, z components, respectively of Darcian fluid velocity;
$\mathbf{v}$, Darcian velocity vector;
x, y, z, Cartesian coordinates;
∇, Del operator;
$\bar{\nabla}^2$, $= A^2\partial^2/\partial x^2 + B^2\partial^2/\partial y^2 + \partial^2/\partial z^2$, modified Laplacian operator present in the dimensionless equations.

Greek symbols

β, thermal expansion coefficient;
η, viscosity;
θ, angle of inclination (Fig. 1);
λ, thermal conductivity;
ρ, density;
ψ, vector potential (ψ_1, ψ_2, ψ_3).

Subscripts

f, fluid;
m, solid–fluid mixture;
s, solid;
0, cold surface.

Superscript

$\bar{}$ dimensionless quantity.

1. INTRODUCTION

SINCE Lapwood's [1] paper on the onset of convection in an infinite, homogeneous, isotropic porous, horizontal slab which is heated from below, there has been considerable interest in thermal convection in permeable materials. For example, Lapwood's results have been extended to: (a) the finite amplitude regime [2, 3]; (b) the situation of temperature dependent fluid properties [4, 5], and (c) the situation of anisotropic permeability [6]. Thermal convection in porous media is of fundamental importance in geothermal reservoir dynamics [7, 8] as well as to thermal process in the oceanic crust [9, 10].

The emphasis of this paper is on thermal convection in porous/permeable zones which are laterally confined, such as is the case of a fault or fracture zone within the earth's crust. By providing the main vertical permeability, such zones may be the controlling factor in many geothermal systems. For example, Basin and Range geothermal systems in the western United States appear to be controlled by deep, nearly vertical master faults [11], the Long Valley, California hydrothermal activity is probably controlled by deep caldera ring fractures and much of the surface activity is along faults [12], the East Mesa, California anomaly

appears to be due to hot fluid rising along a number of active faults [13], and it is apparent that marine hydrothermal circulation is partially concentrated by fault zones [14]. Fault zones may also act as a source to feed shallow horizontal aquifers [15].

Thermal convection in a fault zone may be treated on the basis of convection in a water-saturated, closed, rectangular porous container in which one horizontal dimension is much shorter than the vertical and the other horizontal dimension. There have been several studies of convection in closed containers with a square horizontal plan form [16–22]. Because of the assumptions of insulated vertical walls and square plan geometry, however, these results may not be directly applicable to the problem treated here. Nevertheless, these studies have shown several features of convection in closed containers which are of interest to the problem to be considered. Beck [16] has done the stability analysis for the onset of convection. The later papers have examined the problems of whether two or three dimensional motion occurs at supercritical Rayleigh number, whether the cell at a given Rayleigh number is unique, and whether it is steady. The results indicate that for cubic boxes at a high Rayleigh number the flow may be either 2- or 3-dim., steady or oscillatory depending upon the initial conditions [21], that box dimensions may determine whether 2-dim. or 3-dim. motions exist above a certain Rayleigh number for non-cubic boxes [19, 20], and that for certain box dimensions multiple 3-dim. steady states may exist [22].

On the other hand, studies of convection in closed containers with fault-like geometry [23–28] and with boundary conditions more appropriate to the geological situation are far less complete, particularly as regards the convective motions at finite amplitude. Calculations on the onset of convection in containers with fault-like geometry have been made under the assumption of: (1) insulated side walls [16], in which case the cell pattern was found to take the form of rolls with axes perpendicular to the strike of the fault (transverse rolls); (2) prescribed wall temperatures [24, 25] in which the cell pattern was found to be a single roll with its axis parallel to the strike of the fault (longitudinal roll) and (3) imperfectly conducting side walls [27] in which transverse rolls were assumed *a priori*. The only finite amplitude results [28] assumed an upward through-flow from the base of the fault and assumed the motion to be independent of the coordinate along the strike of the fault; a fixed temperature gradient was maintained along the walls of the fault.

In this paper we investigate some aspects of finite amplitude convection in a rectangular porous container with fault-like geometry. Figure 1 depicts a simple model of a porous fault zone imbedded between two impermeable blocks of material having finite thermal conductivity, and inclined at an angle θ to the vertical. In the cases discussed below, θ was taken to be 90° so that the acceleration of gravity, g, acted in the negative x direction; the y direction was parallel to the strike of the fault zone; the z axis was perpendicular to the strike. By considering the blocks adjacent to the fault zone in which conductive heat transfer to and from the porous zone was allowed to take place, the conditions were more representative of the conditions within the earth's crust; however, we also modeled a few cases in which those blocks were ignored and the x–y planes bounding the fault had a prescribed uniform vertical thermal gradient. In all cases, all of the fault boundaries were assumed to be impermeable; and the x–z planes which bounded the model were assumed to be insulated. The x–y planes bounding the exterior of the models had a prescribed uniform thermal gradient.

The equations were represented in finite difference form; and, subject to various initial conditions, Rayleigh numbers and box aspect ratios, the system was allowed to evolve in time. The outputs for many of the cases modeled were snapshots of slowly evolving solutions. Such outputs were suitable for showing the effect of initial conditions on the subsequent convective flow over time scales of geophysical interest. The results presented below, however, were not sufficient to indicate conclusively whether the final state would have been steady or oscillatory, or whether there may be multiple steady states.

The results were also discussed in the light of limited data from known geothermal systems in which fractures and faults appear to be dominant controlling structures.

2. BASIC EQUATIONS

The pertinent equations of conservation of mass, momentum and energy for the porous zone were, respectively:

$$\nabla \cdot \mathbf{v} = 0, \tag{1}$$

the fluid which is assumed to be incompressible;

$$\mathbf{v} = -(K/\eta)(\nabla P - \rho_f \mathbf{g}), \tag{2}$$

inertial terms being neglected; and the heat transport equation,

$$(\rho c)_m \partial T/\partial t = \lambda_m \nabla^2 T - \rho_f c_f \mathbf{v} \cdot \nabla T. \tag{3}$$

In the impermeable material, heat was transferred by conduction only. Thus

$$\nabla^2 T = (\rho_s c_s/\lambda_s)\partial T/\partial t. \tag{4}$$

Solutions to equations (1)–(4) were subject to boundary conditions. The boundaries of the fault zone were assumed to be impermeable, thus the velocity conditions were

$$\mathbf{v} \cdot \hat{n} = 0 \tag{5}$$

at the boundaries of the porous zone, where n is a unit vector normal to the walls. The top and bottom planes were assumed to be isothermal, thus

$$T = T_1 \quad \text{at } x = 0, \qquad T = T_0 \quad \text{at } x = L_x \tag{6}$$

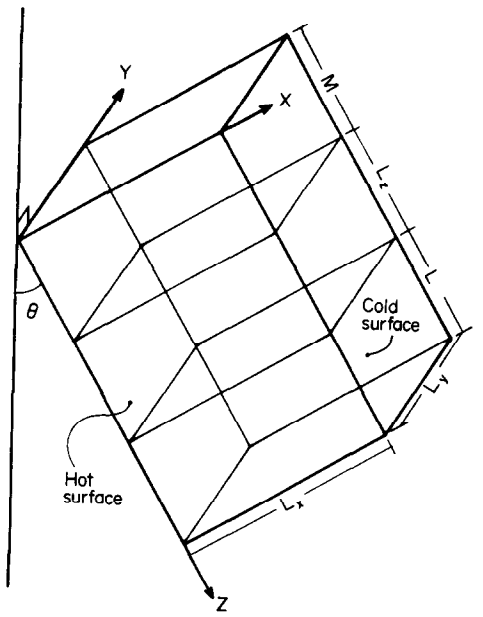

FIG. 1. Basic physical system with its dimensions and temperature boundary conditions.

where $T_1 > T_0$; whereas the vertical boundaries to the extremities of the fault perpendicular to its strike were assumed to be insulated, thus

$$\partial T/\partial y = 0 \quad \text{at} \quad \begin{matrix} y = 0 \\ y = L_y \end{matrix}, \tag{7}$$

and the other vertical boundaries were held at a uniform vertical temperature gradient

$$T = T_1 - (T_1 - T_0)(x/L_x) \quad \text{at } Z = 0 \quad \text{and} \quad M + L_z + L. \tag{8}$$

In some cases the impermeable rock adjacent to the fault was ignored and (8) was applied to the appropriate boundaries of the porous zone. Finally, the fluid density was governed by an equation of state

$$\rho_f = \rho_0[1 - \beta(T - T_0)] \tag{9}$$

which was substituted into the buoyancy term in (2) (i.e. the Boussinesq approximation).

2.1. *Non-dimensionalization and the vector potential*

Holst and Aziz [17] and Horne [21] have shown that the solution to the above equations by finite differences is facilitated by introducing a vector potential rather than by formulating the equations in terms of pressure. We follow their lead by:

(a) introducing a vector potential $\psi = (\psi_1, \psi_2, \psi_3)$, defined by

$$\mathbf{v} = \nabla x \psi, \quad \nabla \cdot \psi = 0; \tag{10}$$

(b) taking the curl of equation (2) to eliminate the pressure

(c) non-dimensionalizing the resulting equations, as well as the heat transport equations (3) and (4), by introducing

$$Q = \frac{\lambda_m}{L_z c_f \rho_0}, \quad T = T_0 + \Delta T_0 T', \quad t = \frac{L_z^2 (\rho c)_m t'}{\lambda_m};$$

$$x = x' L_x, \quad y = L_y y', \quad z = L_z z';$$

$$u = Q u', \quad v = \frac{L_y}{L_x} Q v', \quad w = \frac{L_z}{L_x} Q w';$$

$$\psi_1 = \frac{L_y L_z}{L_x} Q \psi'_1, \quad \psi_2 = L_z Q \psi'_2, \quad \psi_3 = L_y Q \psi'_3.$$

In the porous zone the final, dimensionless equations were

$$\bar{\nabla}^2 T' - A[u'(\partial T'/\partial x') + v'(\partial T'/\partial y') + w'(\partial T'/\partial z')] = \partial T'/\partial t', \tag{11}$$

$$\bar{\nabla}^2 \psi'_2 = -AR\partial T'/\partial z', \tag{12}$$

$$\bar{\nabla}^2 \psi'_3 = AB^2 R \partial T'/\partial y', \tag{13}$$

$$u' = \partial \psi'_3/\partial y' - \partial \psi'_2/\partial z', \tag{14}$$

$$v' = -\partial \psi'_3/\partial x', \tag{15}$$

$$w' = \partial \psi'_2/\partial x' \tag{16}$$

where $R = \rho_0^2 g \beta c_f \Delta T_0 L_x K/\lambda_m \eta$ is the Rayleigh number. In the final form of the equations $\psi'_1 = 0$ because of the assumption that $\theta = 90°$ [17]. In the conducting regions bounding the porous zone, the heat conduction became

$$\bar{\nabla}^2 T' = D\partial T'/\partial t' \tag{17}$$

where

$$D = \rho_s c_s \lambda_m / \rho_m c_m \lambda_s. \tag{18}$$

2.2. *Method of solution*

Equations (11)–(17) together with the appropriate dimensionless boundary conditions were solved numerically by the method of finite differences. Within the porous zone, the equations were solved on an $11 \times 11 \times 11$ grid. The impermeable blocks on each side of the porous zone were of the same dimensions as the porous region and were also represented by $11 \times 11 \times 11$ grids. The energy equation (11) was solved using an explicit, forward time stepping procedure. In this procedure, care must be taken to restrict the size of the time step so that the solution remains numerically stable. Moreover, the advective terms must be treated in a special manner in order to conserve energy within the system. We selected the time step and an energy conserving form of the equations given by Torrance [29]. The Poisson's equations (12) and (13) were solved by the method of successive over-relaxation [30]. To increase the rate of convergence and to minimize the accumulation of errors in the corners, successive scans were begun from different corners of the grid as suggested by Elder [31]. Finally, it was required that temperature and heat flow be continuous across the permeable/impermeable boundary. The finite differ-

ence expressions of these continuity conditions were derived from Carnahan *et al.* [32]. A typical run on a CDC CYBER 74 for a model with $A = B = 0.1$ took about 1800 s CPU time for about 250 time steps. Models with a smaller aspect took ratio considerably longer. Further details of the numerical procedure are given in Hernandez [33].

3. RESULTS

The procedure was to first select a wall boundary condition and an aspect ratio, A and B being taken to be equal. Then, for a fixed Rayleigh number, a variety of initial conditions was chosen. The temperature distribution and the velocity components were printed at specified time intervals throughout the course of the numerical procedure so that the temporal evolution of the cell pattern could be monitored for the different initial velocity perturbations. We have represented the cell pattern by displaying computer-drawn velocity vectors at each grid point on three exterior surfaces of the porous zone, and we have represented the temperature structure by a computer generated 3-dim. schematic of the surface heat flow. The heat flow schematics were shown because the flow patterns on the x–y planes bounding the porous zone were found to be dissimilar for many of the models. This asymmetry across the aperture of the fracture may be observed as an asymmetry in the heat flow anomaly. In the interest of compactness, only the output for the final iteration time is presented in this paper. Results for some intermediate times and for velocity patterns on other representative planes are given in Hernandez [33], as are some other model results. Due to limitations on computer time, several of the models were not allowed to run to a steady state. The calculations were continued until a real time, given reasonable geophysical parameters, of approx. 10^4 yr. Since the magnitude of the time step was subject to change between successive iterations, so that numerical stability could be assured, the runs were not all of identical length. Another criterion for ceasing the calculation was that the flow pattern appeared to vary slowly and regularly from one iteration to the next.

A time of 10^4 yr was chosen as being a time frame on which the system might be through to be reasonably unaltered by geological and geochemical processes (e.g. opening of new permeability by tectonic displacement, clogging by precipitates from the hydrothermal solution). This time scale is just a guess, but it is certainly clear that fracture convection systems in the earth's crust are not likely to exist indefinitely. For all the models, Rayleigh numbers were chosen to be 5 or 10 times the critical number R_c, where R_c was taken from the work of Shyu [26] for a fracture of a given aspect ratio and prescribed wall temperatures along the x–y boundary planes.

The convection was initiated by placing a small upward velocity perturbation at different locations, referred to below as (I), (II) or (III), along the base of the porous zone. Condition (I) refers to a perturbation at (0, 0, 0); condition (II) refers to a perturbation placed at (0, 2, 0) and (0, 9, 0); condition (III) refers to a perturbation placed at (0, 0, 5) and (0, 10, 5), where the coordinates refer to grid points defined within the porous zone. The magnitude of the perturbation was about two orders of magnitude smaller than the maximum of the x component of the velocity at the end of the calculations. The significance of the form of the initial conditions was that (I) and (II) were asymmetric with respect to the fracture aperture whereas (III) was symmetric. Condition (II) would tend to produce longitudinal rolls whereas (III) would tend to produce transverse rolls. There is no clear, precise physical significance to the form of the initial conditions chosen, although (II) might be envisioned as resulting from displacement of the fault walls during tectonic activity (e.g. normal faulting), and (III) might be envisioned as a response to tidal forces.

In order to make the conversion to dimensional time, $L_z = 10^3$ m for $A = B = 0.1$; $L_z = 10^2$ m for $A = B = 0.01$; $(\rho c/\lambda)_m = 10^{-6}$ m^2/s.

3.1. *Prescribed wall temperatures*

Figures 2 and 3 show the cell pattern and surface heat flux for situations in which $R = 5R_c$, $A = B = 0.1$, and the perturbation was (I) and (II), respectively. The velocity field indicates a 3-dim. flow pattern; however, the velocity across the fracture aperture is considerably smaller than the other two components. Thus, the flow consists mainly of 2-dim transverse rolls in which the fluid rises along the two insulated walls and sinks at the center. There are some small secondary cells, and the velocity vectors along the planes shown suggest that there may in fact be two pair of rolls, one in the upper part of the fault and one in the lower. A print-out of the flow pattern on other planes shows that this is not the case, however [33]. The heat flow anomaly further indicates that the flow pattern is symmetric across the width of the fault, despite the fact that the initial perturbations were asymmetric in both cases. The calculations were run for a real time of 12,000 yr. The pattern in both cases was essentially unchanged for several thousand years preceding the final output. The results suggest that at $R = 5R_c$, the flow pattern in faults with prescribed wall temperatures should take the form of transverse rolls regardless of the initial condition. Calculations done at $R = 10R_c$ with symmetric initial perturbations gave essentially the same result [33].

3.2. *Imperfectly conducting walls*

For these cases, blocks of impermeable rock with a finite thermal conductivity and with the same dimensions as the porous zone were placed in a manner as indicated in Fig. 1. Figures 4–7 show the convection pattern and heat flow for cases with aspect ratios $A =$

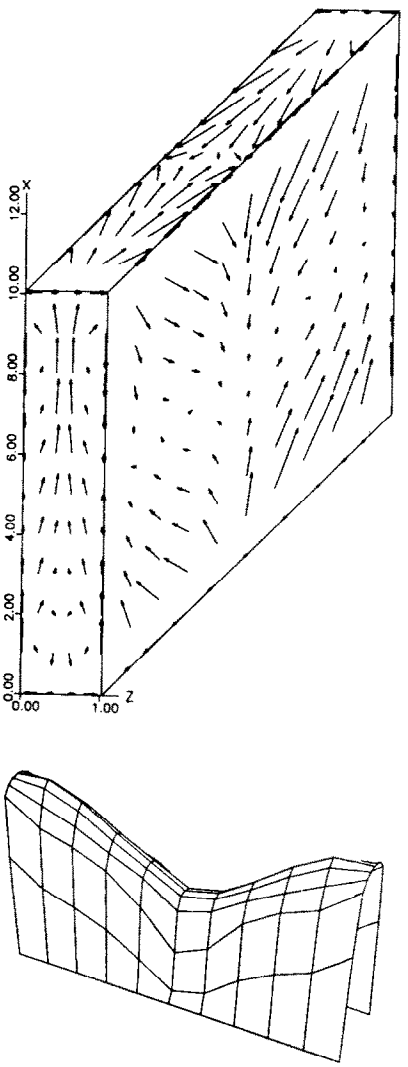

FIG. 2. Flow pattern and surface heat flow anomaly for fault zone assuming faces $z = 0$ and $z = 1$ have a prescribed temperature gradient. $R = 5R_c$, $A = B = 0.1$, $t = 12{,}000$ yr. Initial perturbation: asymmetric, type (I).

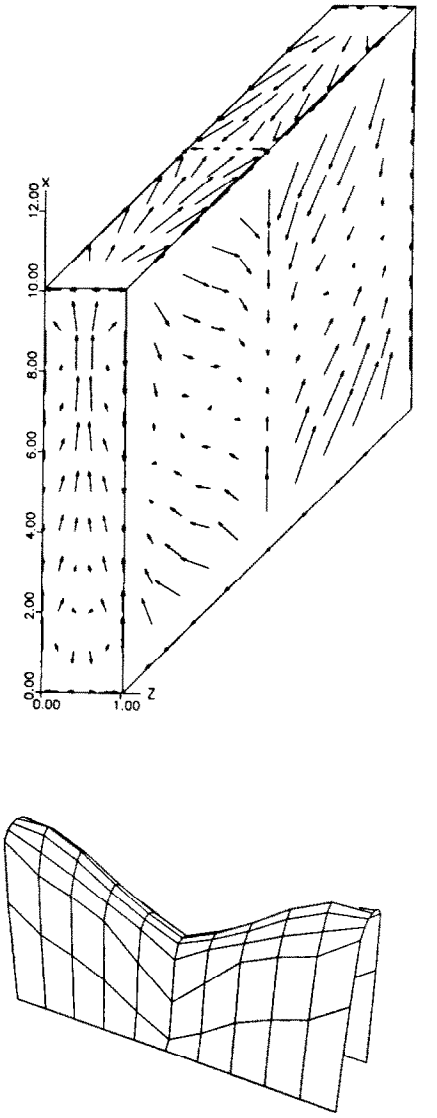

FIG. 3. Same model as Fig. 2 except initial perturbation was asymmetric, type (II).

$B = 0.1$, but for different Rayleigh numbers and initial perturbations.

Figure 4 shows the situation after a computation time corresponding to 7500 yr, assuming a Rayleigh number $R = 5R_c$ and a type (I) perturbation. It is clear that the flow is much more irregular than in the cases with prescribed wall temperatures. There is a pronounced tendency toward the development of a transverse roll at the end of the zone far from the initial perturbation; however, the circulation near the end where the perturbation was initiated shows evidence of two cells, one of which has a longitudinal character (see plane $y = 0$, Fig. 4). The asymmetry of the convection pattern is quite evident in the heat flow schematic. Moreover, there is a substantial heat flow anomaly across the upper surface of the impermeable zone. This indicates that heat is transferred laterally through the fault boundaries and the excess heat is conducted through the upper surface. The asymmetry further suggests that the conductive heat transfer across the impermeable/permeable boundaries parallel to the strike of the fault is strongly influenced by the initial perturbation.

Figures 5 and 6 show the situation assuming $R = 5R_c$ and $R = 10R_c$, respectively. An initial perturbation of type (III) was used. Such a perturbation would be expected to induce transverse rolls; and, ignoring the small secondary cells and the small horizontal component of velocity across the width of the fault, transverse rolls are mainly what is observed. Although the outputs shown are for 12,000 and 7000 yr, respectively, samples at earlier times show that the circulation was developed by 3000 yr and has been steady since.

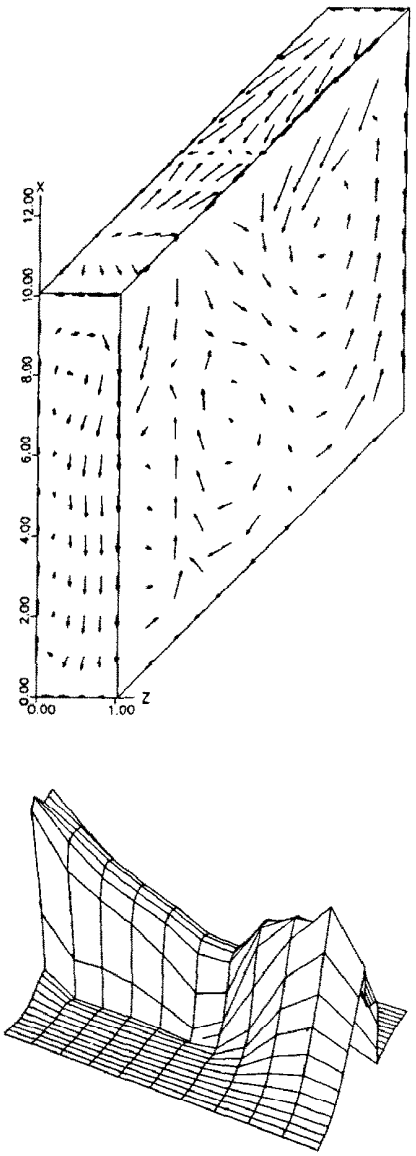

FIG. 4. Flow pattern and surface heat flow anomaly for a fault zone assuming faces $z = 0$ and $z = 1$ are in contact with impermeable material of finite thermal conductivity. $R = 5R_c$, $A = B = 0.1$, $t = 7500$ yr. Initial perturbation: asymmetric, type (I).

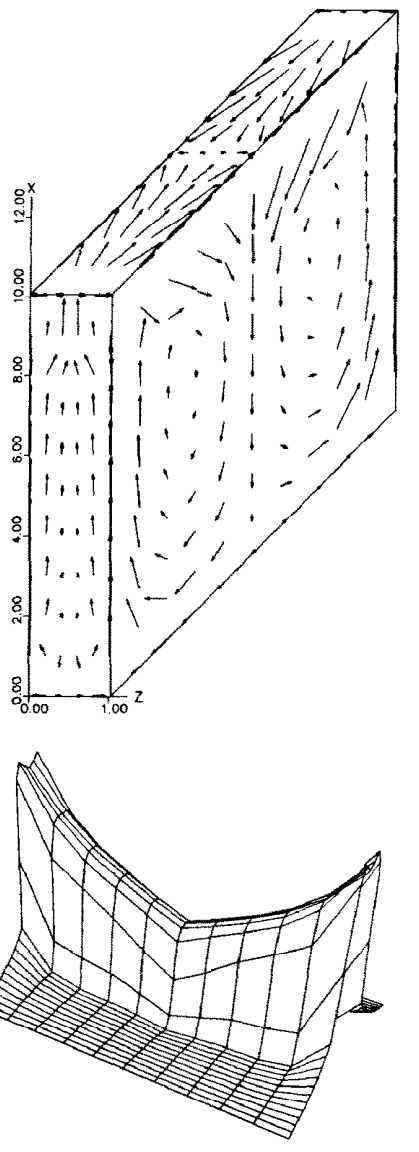

FIG. 5. As in Fig. 4 except $t = 12{,}000$ yr and initial perturbation was symmetric, type (III).

Figure 7 shows the situation after 13,500 yr assuming $R = 10R_c$ and an initial perturbation of type (II). Such a perturbation would tend to induce a longitudinal roll; however, the plan form indicated by the planes $x = 1$, $z = 1$ in the figure suggests a pair of transverse roll; however, the plan form indicated by the planes $x = 1$, $z = 1$ in the figure suggests a pair of transverse in the plane $y = 0$ are somewhat suggestive of a longitudinal roll, and the plane $z = 0$ (not shown, see Hernandez [33]) consists mainly of an ascending sheet. The heat flow schematic also indicates the high degree of asymmetry. A heat flow profile along the strike of the fault zone would indicate a pattern corresponding to transverse rolls; whereas a profile perpendicular to the strike, particularly near the ends of the fault would show a marked cross-strike heat flow gradient. Quite evidently, as a consequence of heat transfer into the impermeable material, the initial perturbation has executed a significant control on the subsequent development of the convection pattern.

Figures 8 and 9 show two examples of the convection pattern and surface heat flow for models in which the aspect ratio was $A = B = 0.01$. Figure 8 is for $R = 10R_c$ and an initial perturbation of type (III). As in the previous cases in which such a perturbation was used Figs. 5, 6), the fluid convects basically as a pair of transverse rolls. Figure 9 is for $R = 5R_c$ and an initial perturbation of type (II). In this case, the flow pattern is more strongly indicative of transverse rolls than in the corresponding model with the higher aspect ratio (Fig. 7). The heat flow schematic, however,

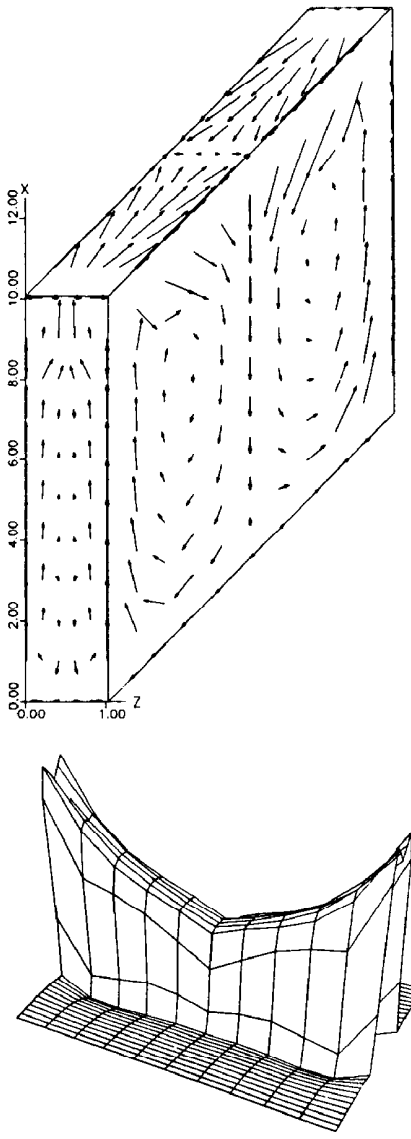

FIG. 6. As in Fig. 5 except $R = 10R_c$, $t = 7000$ yr.

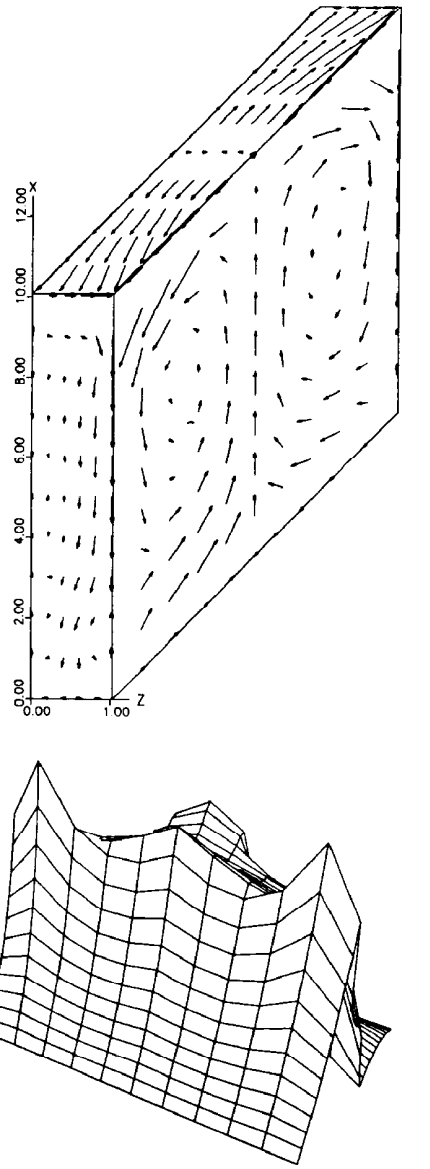

FIG. 7. As in Fig. 4 except $R = 10R_c$, $t = 13{,}500$ yr, and initial perturbation was asymmetric, type (II).

shows an asymmetry perpendicular to the strike of the fracture which is in some ways similar to that shown in Fig. 7. Once again, because of the finite thermal conductivity of the impermeable material adjacent to the fault, the asymmetric initial condition tends to affect the subsequent evolution of the flow.

4. DISCUSSION AND CONCLUSIONS

4.1. *The cell pattern*

The main purpose of this study was to investigate, to a limited degree, the effects of initial and boundary conditions on finite amplitude convection in a porous container with fault-like geometry. Earlier work of Lowell and Shyu [25] has shown that at the onset of convection in a fault zone with prescribed wall temperatures the cell pattern should be of the form of a longitudinal roll; but they suggested that at finite amplitude that 3-dim. convection might be more likely. They also raised the question as to whether in a fault zone bounded by impermeable walls of finite thermal conductivity the flow might evolve in time to a flow which might be typical of an insulated wall boundary condition. In addition, the work done on finite amplitude convection in cubic containers with insulated walls has indicated that the flow may be either 2- or 3-dim. and dependent upon the initial conditions [19–22].

Our results can be summarized as follows:

(1) In models with prescribed wall temperatures, the flow was steady, symmetric, and weakly 3-dim. regardless of whether the initial perturbation was symmetric or asymmetric. Thus, the suggestion of [25] that the finite amplitude flow might be 3-dim., even though longitudinal rolls occur at $R = R_c$, was affirmed. Since the transverse velocity component was small, however,

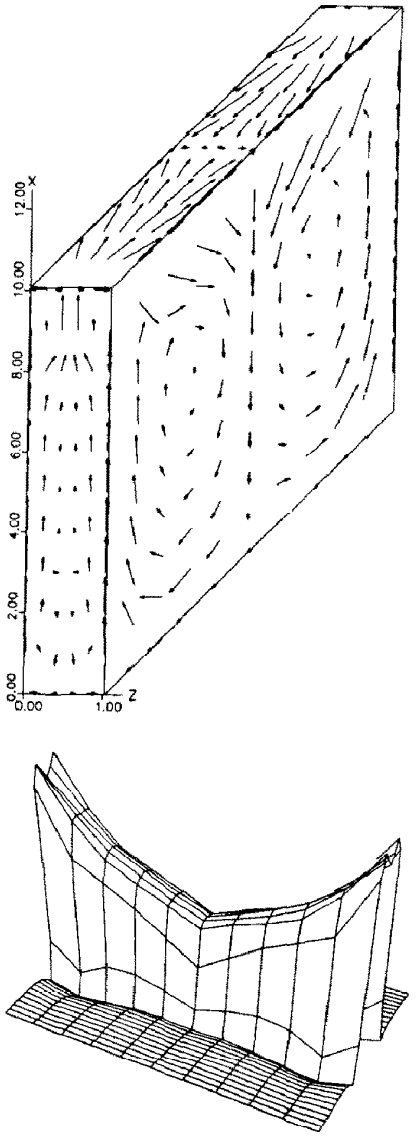

FIG. 8. As in Fig. 6 except t = 6000 yr, $A = B = 0.01$.

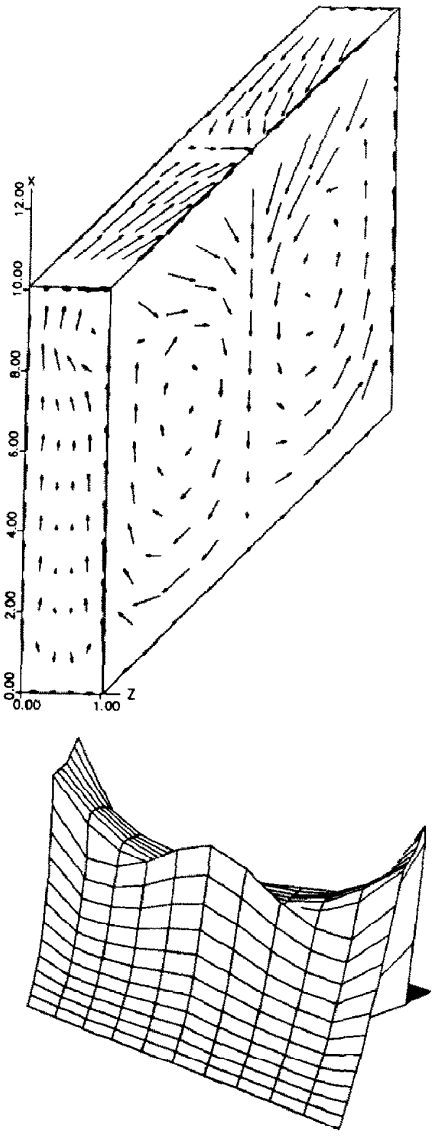

FIG. 9. As in Fig. 7 except $R = 5R_c$, $A = B = 0.01$.

the surface heat flow anomaly gave the appearance of 2-dim. transverse rolls. The results did not appear to depend upon the Rayleigh number in the range $5R_c \leq R \leq 10R_c$.

(2) In models bounded by impermeable slabs of finite thermal conductivity, the flow pattern was dependent upon the form of the initial perturbation. Models in which the initial perturbation was symmetric [type (III)] set up steady, symmetric cell patterns which, though weakly 3-dim., basically took the form of transverse rolls. Such a pattern developed for $R = 5R_c$ or $10R_c$ and aspect ratios of 0.1 or 0.01. Based on the heat flow anomaly calculation, there was very little heat transfer out of the porous zone. The heat flow anomaly varied along the strike of the fault, corresponding to the regions of rising and sinking flow in the expected manner.

On the other hand, when the initial perturbation was asymmetric [(I) or (II)], the resulting convective flow tended to retain the asymmetry for a time of at least several thousand years. Because of the expense involved in making these calculations, especially for the models with aspect ratio of 0.01, the calculations were not run to an equilibrium state, if in fact there was one. We had expected that the effect of heat transfer across the walls of the fault would be to render those walls insulators as the convection pattern evolved. The resulting pattern would then have been similar to that arising from a symmetric initial perturbation. There is some evidence that this was indeed what was developing. Figures 7 and 9 show considerable similarity to the transverse rolls in Figs. 6 and 8, particularly in the plane $z = 1$. The long-strike heat flow anomaly in Figs. 7 and 9 is also consistent with much of the flow within the fault zone being characterized by transverse rolls.

Based on these limited results, it appears that finite amplitude convection in a fault zone, whether with prescribed wall temperatures or with finite heat trans-

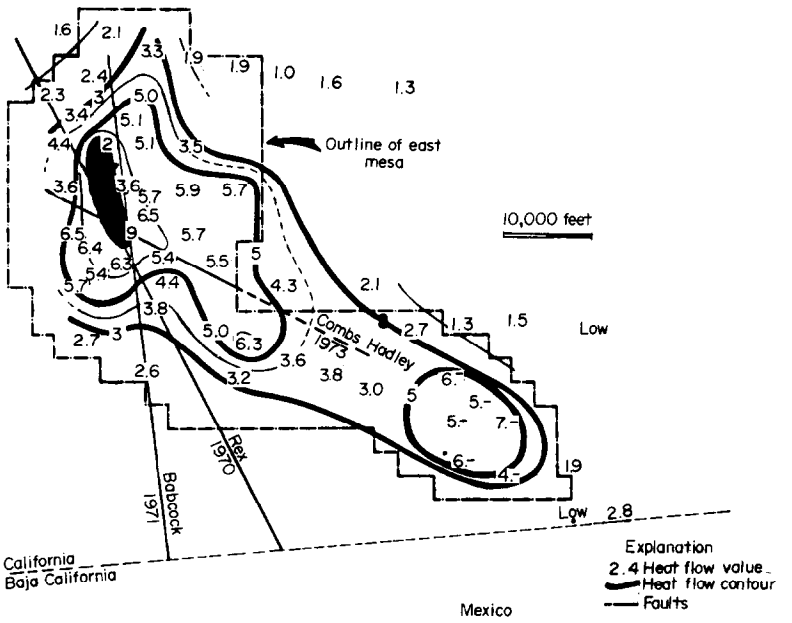

FIG. 10. Distribution of the heat flow over the East Mesa heat flow anomaly and Border anomaly (Southeast Lobe). Data from Swanberg [13].

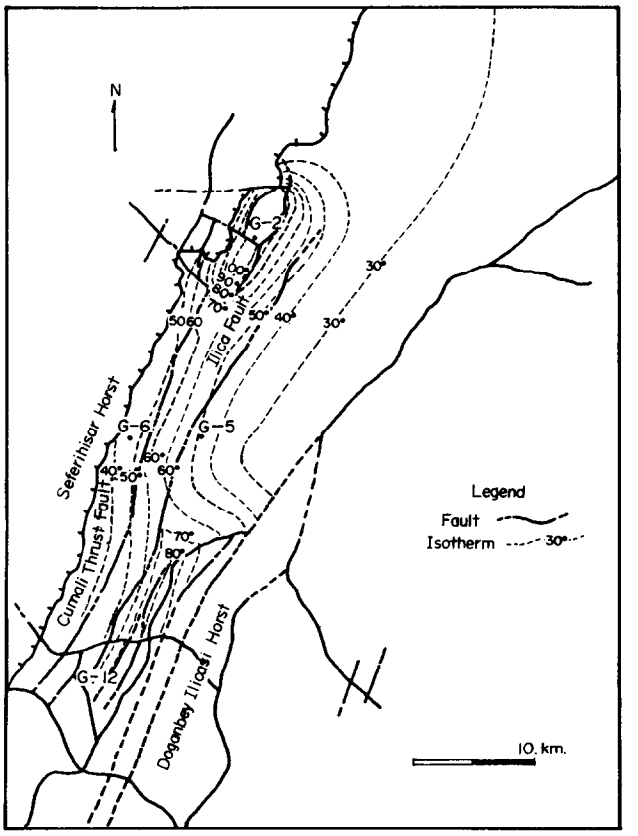

FIG. 11. Isotherm contour map for 100 m depth inside the Graben-I in the Izmir-Seferihisar area. Data from Esder and Sinsek [34].

fer, tends to be a weakly 3-dim. flow in which the dominant mode is transverse rolls. These results hold for Rayleigh numbers up to 10 times critical.

More work is needed to determine whether steady transverse rolls really do develop at long times in systems with finite heat transfer across the walls of the fault, whether the patterns that have evolved are stable, whether there may be other steady states etc. Intuitively, it would seem that the cubic plan form, insulated boundary models which have been studied to date may admit a broader range of solutions than would be possible in the models with fault-like geometry and with finite or infinite heat transfer boundary conditions which we have studied.

It is interesting to note that for times of the order of 10^4 yr, the effect of asymmetric initial perturbations may still be observed by the fact that the heat flow anomaly exists well outside the porous zone and that the anomaly is asymmetric across the strike of the fault. This result may be of considerable geophysical importance.

4.2. *Application to known geothermal systems*

Available data on fault-controlled geothermal systems is very sketchy and such systems tend to be geologically complex; so it is difficult to compare the results of our simple model with field data in a quantitative fashion. Two continental thermal areas which appear to be fault controlled are the East Mesa Anomaly in the Imperial Valley, California and the Izmir-Seferihisar Area in Western Turkey. Figures 10 and 11 show that for each of these areas an alternating pattern of thermal highs and lows follows the linear trend of the fault zones. The spatial scales are of the order of a few kilometers for each area. The thermal pattern may be due to ascending and descending fluid associated with transverse convective rolls within the fault zone — perhaps as are indicated by Figs. 5, 6, or 8 of the model results. The absence of any apparent asymmetry across the strike of the fault zones is certainly not conclusive evidence as to the nature of the initial perturbation, since geological as well as physical processes may determine the form of the flow pattern in natural systems. For example, it may well be reasoned that the permeability in fault zones may be anisotropic and that the transverse horizontal permeability is lower than the other components [23]. Such an anisotropy would tend to force transverse rolls rather than longitudinal rolls.

Green [14] has examined a rather detailed suite of heat flow data from the Galapagos Spreading Center. His results suggest a widespread porous medium type hydrothermal circulation with substantial local control of the circulation by escarpments. In fact, a traverse across a section of an escarpment shows a substantial transverse heat flow anomaly gradient with high heat flow on the upthrown side. Green suggests that the circulation is not completely forced by the topography (the chimney effect). Is it possible that convection with the fault zone itself, perhaps partly evolving from an asymmetric, fault motion induced initial perturbation, is partially responsible? Clearly, theoretical models of fault zone convection need to be improved and additional detailed measurements on fault-controlled geothermal systems are necessary.

Acknowledgements—This work was supported by the Extramural Geothermal Program of the United States Geological Survey under Grant No. 14-08-00001-G-540.

REFERENCES

1. E. R. Lapwood, Convection of a fluid in a porous medium, *Proc. Cambridge Phil. Soc.* **44,** 508–521 (1948).
2. J. M. Straus, Large amplitude convection in porous media, *J. Fluid Mech.* **64,** 51–63 (1974).
3. J. W. Elder, Physical processes in geothermal areas, in *Terrestrial Heat Flow*, monogr. 8 (edited by W. H. K. Lee) pp. 211–219. A.G.U. Washington D.C. (1965).
4. D. R. Kassoy and A. Zebib, Variable viscosity effects on the onset of convection in porous media, *Phys. Fluids* **18,** 1649–1651 (1975).
5. J. M. Straus and G. Schubert, Thermal convection of water in a porous medium: effects of temperature- and pressure-dependent thermodynamic and transport properties, *J. geophys. Res.* **82,** 325–333 (1977).
6. R. A. Wooding, Influence of anisotropy and variable viscosity upon convection in a heated, saturated porous layer, Applied Math. Div. Tech. Rept. No. 55, DSIR, Wellington, N.Z. (1976).
7. I. G. Donaldson, The simulation of geothermal systems with a simple convective system, *Geothermics* **2**(1), 649–654 (1970).
8. J. W. Mercer, G. F. Pinder and I. G. Donaldson, A Galerkin-finite element analysis of the hydrothermal system at Wairakei, New Zealand, *J. geophys. Res.* **80,** 2608–2621 (1975).
9. C. R. B. Lister, On the thermal balance of a mid-ocean ridge, *Geophys. J. R. Astr. Soc.* **26,** 515–535 (1972).
10. P. A. Rona and R. P. Lowell (eds.), *Seafloor Spreading Centers: Hydrothermal Systems*, Benchmark Papers in Geol. Vol. 56. Hutchinson Ross, Stroudsburg, Pennsylvania (1980).
11. R. K. Hose and B. E. Taylor, Geothermal systems of Northern Nevada, U.S.G.S. Reports, open-file series, 74–271 (1974).
12. R. A. Bailey, G. B. Dalrymple and M. A. Lanphere, Volcanism, structure and geochemistry of Long Valley caldera, Mono County, California, *J. geophys. Res.* **81,** 725–744 (1976).
13. C. A. Swanberg, The mesa geothermal anomaly, Imperial Valley, California: A comparison and evaluation of results obtained from surface geophysics and deep drilling, In *Proc. Second U.N. Symp. on the Development and Use of Geothermal Resources*, San Francisco **2,** 1217–1229 (1975).
14. K. E. Green, R. P. von Herzen and D. L. Williams, The Galapagos Spreading Center at 86°W: a detailed geothermal field study, *J. geophys. Res.* **86,** 979–986 (1981).
15. K. P. Goyal and D. R. Kassoy, Fault zone controlled charging of a liquid-dominated geothermal reservoir, *J. geophys. Res.* **85,** 1867–1875 (1980).
16. J. L. Beck, Convection in a box of porous material saturated with fluid, *Phys. Fluids* **15,** 1377–1383 (1972).
17. P. H. Holst and K. Aziz, Transient three-dimensional natural convection in confined porous media, *Int. J. Heat Mass Transfer* **15,** 73–90 (1972).
18. A. Zebib and D. R. Kassoy, Three-dimensional natural convection motion in a confined porous medium, *Phys. Fluids* **21,** 1–3 (1977).

19. J. M. Straus and G. Schubert, On the existence of three-dimensional convection in a rectangular box containing fluid saturated porous material, *J. Fluid Mech.* **87**, 385–394 (1978).
20. J. M. Straus and G. Schubert, Three-dimensional convection in a cubic box of fluid saturated porous material, *J. Fluid Mech.* **91**, 155–165 (1979).
21. R. N. Horne, Three-dimensional natural convection in a confined porous medium heated from below, *J. Fluid Mech.* **92**, 751–766 (1979).
22. J. M. Straus and G. Schubert, Modes of finite-amplitude three-dimensional convection in rectangular boxes of fluid saturated porous material, *J. Fluid Mech.* **103**, 23–32 (1981).
23. R. P. Lowell, The onset of convection in a fault zone: effect of anisotropic permeability, *Geothermal Resources Council Transactions* **3**, 377–380 (1979).
24. R. P. Lowell, Convection in narrow vertical fracture spaces, *Final Technical Report*, U.S.G.S. grant no.: 14-08-00001-G-540 (1980).
25. R. P. Lowell and C. T. Shyu, On the onset of convection in a water saturated porous box: effects of conducting walls, *Lett. Heat Mass Transfer* **5**, 371–378 (1978).
26. C. T. Shyu, Numerical analysis of critical field functions for thermal convection in vertical or quasivertical Darcy flow slabs, Ph.D. Thesis, Oregon State University, Corvallis (1979).
27. H. D. Murphy, Convective instabilities in vertical fractures and faults, *J. geophys. Res.* **84**, 6234–6245 (1979).
28. D. R. Kassoy and A. Zebib, Convection fluid dynamics in a model of a fault zone in the earth's crust, *J. Fluid Mech.* **88**, 769–792 (1978).
29. K. E. Torrance, Comparison of finite-difference computations of natural convection, *J. Res. Nat. Bur. Stand.* **72B**, 281–301 (1968).
30. D. Young, Iterative methods for solving partial difference equations of elliptic type, *Trans. Am. math. Soc.* **76**, 92–111 (1956).
31. J. W. Elder, Numerical experiments with free convection in a vertical slot, *J. Fluid Mech.* **24**, 823–843 (1966).
32. B. Carnahan, H. A. Luther and J. O. Wilkes, *Applied Numerical Methods*. John Wiley, New York (1969).
33. H. Hernandez, Numerical modeling of the convection in a fault zone, M.S. Thesis, Georgia Institute of Technology, Atlanta (1980).
34. T. Esder and S. Simsek, Geology of Izmir-Seferihisar geothermal area, Western Anatolia of Turkey; determination of reservoirs by means of gradient drilling, In *Proc. Second U.N. Symp. on the Development and Use of Geothermal Resources*, San Francisco **1**, 349–361 (1975).

CONVECTION D'AMPLITUDE FINIE DANS UN VOLUME POREUX AVEC UNE GEOMETRIE DE FAILLE: EFFET DES CONDITIONS INTIALES ET AUX LIMITES

Resumé—On utilise les techniques de différences finies pour étudier la convection d'amplitude finie dans un volume poreux avec une géométrie de faille. Le but principal est la détermination du rôle des conditions limites aux parois et de la perturbation initiale sur la configuration d'écoulement. Dans des volumes avec des températures données à la paroi, l'écoulement est faiblement tridimensionnel, avec l'apparence générale de rouleaux transverses bidimensionnels. Dans des volumes limités par des blocs imperméables à conductivité thermique finie, il s'établit une configuration d'écoulement proche de celle relative aux volumes avec températures de paroi fixées; mais des perturbations initiales dissymétriques tendent á faire apparaître des écoulements dans lesquels des dissymétries sont encore présentes aprés 10^4 ans. Les résultats sont comparés avec des données relatives à des systèmes géothermiques existants dans la nature.

KONVEKTION MIT ENDLICHER AMPLITUDE IN EINEM PORÖSEN BEHÄLTER MIT VERWERFUNGSARTIGER GEOMETRIE: EINFLUSS DER ANFANGS- UND RANDBEDINGUNGEN

Zusammenfassung—Differenzenverfahren wurden angewandt, um die Konvektion mit endlicher Amplitude in einem porösen Behälter mit verwerfungsartiger Geometrie zu untersuchen. Das Hauptziel bestand darin, die Rolle der Randbedingungen an der Wand und die der anfänglichen Ungleichförmigkeit auf die spätere Strömungsverteilung zu ermitteln. In Behältern mit vorgegebenen Wandtemperaturen war die Strömung schwach dreidimensional, es traten aber ständig zweidimensionale Querwalzen auf. In Behältern, die von undurchlässigen Blöcken endlicher Wärmeleitfähigkeit begrenzt waren, zeigte die Strömungsverteilung die Tendenz zu einem ähnlichen Verhalten wie bei den Behältern mit vorgegebenen Wandtemperaturen, jedoch führten asymmetrische anfängliche Ungleichförmigkeiten zu langsam sich entwickelnden Strömungen, in denen Asymmetrien noch nach 10^4 Jahren vorhanden waren. Die Ergebnisse wurden mit den Daten natürlich auftretender geothermischer Systeme verglichen.

КОНВЕКЦИЯ КОНЕЧНОЙ АМПЛИТУДЫ В ПОРИСТОМ ОГРАНИЧЕННОМ ОБЪЕМЕ НЕСОВЕРШЕННОЙ ГЕОМЕТРИИ. ВЛИЯНИЕ НАЧАЛЬНЫХ И ГРАНИЧНЫХ УСЛОВИЙ

Аннотация — Конвекция конечной амплитуды в пористом ограниченном объеме несовершенной геометрии исследовалась методом конечных разностей. Основная цель исследования состояла в определении влияния граничных условий на стенке и начального возмущения на картину течения. При заданных значениях температуры стенок наблюдается почти трехмерный поток с двумерными поперечными валами, возникающими по всему объему. В объемах, ограниченных непроницаемыми стенками конечной теплопроводности, наблюдается аналогичная картина течения, но асимметричные начальные возмущения вызывают медленно развивающееся течение, асимметрия которого еще наблюдается через 10^4 лет. Проведено сравнение полученных результатов с данными для природных геотермальных систем.